^{13}C Nuclear Magnetic Relaxations and Chain Local Motions of Poly(vinyl chloride) in Dibutyl Phthalate and Tetrachloroethane Solutions

T. Radiotis and G. R. Brown*

Department of Chemistry, McGill University, 801 Sherbrooke Street West, Montréal, Québec, Canada H3A 2K6

Photis Dais*

Department of Chemistry, University of Crete, P.O. Box 1470, 71409 Iraklion, Crete, Greece

Received September 25, 1992; Revised Manuscript Received December 1, 1992

ABSTRACT: Carbon-13 spin–lattice relaxation times and NOE values were measured as a function of temperature at two magnetic fields for poly(vinyl chloride) (PVC) in two solvents, dibutyl phthalate (DBP) and 1,1,2,2-tetrachloroethane-d_2 (TCE-d_2). The relaxation data were interpreted in terms of chain local motions by using various dynamic models. Among these, the Dejean–Lauprêtre–Monnerie correlation function appears to be the most appropriate to describe the chain segmental motions of PVC. Simulation parameters from this model were found to differ for PVC in the two solvents; e.g., the half-angles of the librational motion of the C–H vector for the methine carbon were found to be 27 and 30° in DBP and in TCE-d_2, respectively. This can be rationalized by assuming a specific interaction between DBP and the CHCl group of PVC. In addition, the activation energies for cooperative segmental motions were found to be 9.2 kJ/mol for PVC in DBP as compared to 13.7 kJ/mol when the polymer is in the TCE-d_2 solvent. This difference can be attributed to effects that arise from the relative solvent quality.

Introduction

In recent years considerable effort has been devoted to the study of macromolecular dynamics as determined from ^{13}C nuclear magnetic relaxation parameters. The main advantage of this spectroscopic technique is that it provides a detailed analysis of molecular motion at the atomic level. Several reviews[1–5] are available describing the various models developed for the interpretation of nuclear spin relaxation data for polymers in solution.

Initial attempts to quantitatively interpret polymer dynamics led to the use of distribution models and especially the so-called log χ^2 distribution of Schaefer.[6] This model utilizes a broad asymmetric distribution of correlation times for the molecular motions with a tail toward the high end of the scale; however, it lacks the detailed insight into the nature of the chain motions. More promising models have been developed which are based on a molecular description of segmental motions. These include the three-bond jump model developed by Jones and Stockmayer[7] (JS model) and the conformational jump model of Hall, Weber, and Helfand[8,9] (HWH model). Recently, Dejean, Lauprêtre, and Monnerie[10] (DLM model) modified the HWH model by taking into consideration a fast libration of the C–H vectors in addition to segmental motion.

On the basis of the present relaxation data for poly(vinyl chloride) (PVC) in dibutyl phthalate (DBP) and 1,1,2,2-tetrachloroethane-d_2 (TCE-d_2), a critical evaluation of these four models will be made regarding their ability to describe the local motions of the PVC chain. In addition, a comparison of the dynamics of PVC in the two solvents will be made in search of discernible differences in local motion, apart from the effects of solvent viscosity.

The goal of this study was to obtain insight into the chain local motions of PVC dissolved in DBP, a phthalate diester. Such studies are important from an academic as well as an industrial point of view since phthalates are used extensively as primary plasticizers, to convert the rigid PVC resin into workable and flexible compounds that exhibit a wide range of properties depending on the type and concentration of plasticizer. Although the technology of plasticization is well developed,[11,12] the mechanism of plasticization of PVC and its interactions with the plasticizer are not well understood at the molecular level. For comparison, a parallel study was made for solutions of PVC in TCE-d_2.

Experimental Section

Polymer. The poly(vinyl chloride) used in this study was an Esso 366 industrial resin for which the following characteristics were quoted: $\bar{M}_n$ = 46 000; $\bar{M}_w$ = 83 000; density = 1.39 g/cm^3 and $[\eta]$ = 0.98 dL/g in chlorobenzene at 25 °C. The glass transition temperature, T_g, as determined by a Perkin-Elmer DSC-2C was 87 °C. Prior to use the PVC sample was dissolved in THF and precipitated with cold methanol in order to remove impurities and low molecular weight species. Studies by ^{13}C NMR indicated an essentially atactic polymer with P_m = 0.45, as determined from the methine triad sequence distribution.

Viscosity. Viscosity measurements were carried out by means of calibrated Ubbelodhe-type viscometers having various capillary sizes (SGA Scientific Inc.) immersed in a thermostated water bath, regulated to ±0.02 °C. Dilute solutions of PVC in DBP (0.06–0.20 g/dL) and in TCE (0.04–0.20 g/dL) were prepared with solvents purchased from Aldrich Co. All viscosity measurements were repeated at least twice. The effect of concentration on the viscosity of dilute polymer solutions can be described by Huggins:[13]

$$\eta_{sp}/c = [\eta] + k_H[\eta]^2 c \tag{1}$$

and Kraemer:[14]

$$\ln(\eta_r)/c = [\eta] + k_K[\eta]^2 c \tag{2}$$

where η_{sp} is the specific viscosity, η_r is the relative viscosity, and c is the concentration in g/dL. Values of intrinsic viscosity, $[\eta]$, and Huggins, k_H, and Kraemer, k_K, constants for PVC in DBP at 30 °C were found to be 0.89 dL/g, 0.36, and −0.13, respectively, and 0.74 dL/g, 0.74, and 0.19 for PVC in TCE. Activation energies for the solvent viscosity, ΔH_η, obtained from the slopes of the plots of $\ln(\eta)$ as a function of $1/T$ were found to be 24.2 and 10.2 kJ/mol in DBP and TCE, respectively, over the temperature range 20–90 °C.

NMR. In the NMR experiments, the polymer was studied as 5% w/v solutions in both DBP (Aldrich Co.) and TCE-d_2 (MSD

0024-9297/93/2226-1445$04.00/0

Isotopes). The lock signal for the PVC solution in the protonated DBP solvent was obtained either by using an external tube containing a solution of DBP in TCE-d_2 or by placing a coaxial tube containing deuterated solvent inside the 10-mm tube. No differences in relaxation parameters were observed by using these two techniques.

Carbon-13 spin–lattice times, T_1, and nuclear Overhauser enhancements, NOE, values were measured using Varian XL-200 and XL-300 spectrometers operating at 50.3 and 75.4 MHz, respectively, for the carbon nucleus. The temperature was controlled to within ±0.5 °C, as indicated by a precalibrated copper–constantan thermocouple in the probe insert. Spin–lattice relaxation times were measured by the standard inversion recovery method (PD–180°–t_D–90°–AT) with a repetition time longer than $5T_1$. A total of 500–2000 transients, depending on solvent and temperature, was accumulated for each set of 12–14 "arrayed" t_D values. Values of T_1 were determined by a three-parameter nonlinear procedure with a rms uncertainty of less than ±5%. ^{13}C NOE experiments were carried out by reverse gated decoupling, at least three experiments being performed at each temperature. Delays of at least 10 times the longest T_1 were used between the 90° pulses.

Numerical Analysis. The correlation times were calculated using a modified[15,16] version of the MOLDYN[17] program which includes the JS, HWH, and DLM motional models. Experimental relaxation data (T_1 and NOE values) for the methine, CH, and/or methylene, CH_2, carbons of PVC, determined at both field strengths for a given temperature, were used as the input data. Using a Simplex routine, the best fit relaxation data were calculated by varying one or more simulation parameters, depending on the model, until the target function, F, described by eq 3 as the sum of the squares of the relative deviations between the experimental and calculated T_1 and NOE values was a minimum

$$F = \sum_{i=1}^{n}\left[\frac{S_{i,\mathrm{cal}} - S_{i,\mathrm{exp}}}{S_{i,\mathrm{exp}}}\right]^2 \tag{3}$$

where $S = T_1$ and/or NOE, and n represents the number of experimental relaxation parameters. Throughout this paper differences between the experimental and calculated values are described by the function σ, defined as the root mean square of the relative deviations,

$$\sigma = \sqrt{F}/n \tag{4}$$

Initially, calculations using the log χ^2 distribution were performed by entering the relaxation data for the methine carbon, determined at both fields strengths, at the temperature where the T_1 exhibits a minimum value. The optimum correlation time $\bar{\tau}$ was determined by varying the distribution width p, in steps of unity, until a minimum F value was obtained. The methylene relaxation data were then calculated using the optimized values of $\bar{\tau}$ and p from the methine carbon. In the HWH and JS models, T_1 and NOE values of the CH and CH_2 carbons, for both field strengths at a temperature corresponding to the T_1 minimum, were entered simultaneously through a geometry file that included a nonbonded dipolar relaxation mechanism. In the former model, τ_0 and τ_1 were optimized simultaneously, while for the latter model ω_3 was optimized and the parameter $2m - 1$ was varied manually in steps of unity until a minimum F value was obtained. No significant deviations between experimental and calculated relaxation data were found when the data for CH and CH_2 carbons were entered separately or using a geometry file which embodied nonbonded ^{13}C–^1H dipolar interactions.

For the DLM model, relaxation data for the CH carbon at the minimum of the plot of T_1 as a function of $1/T$ were used as input values and the optimized values for the correlation time for cooperative motion τ_1 and the angle θ_{CH} were determined by varying τ_0/τ_1 and τ_1/τ_2 manually in steps of 1 and 10 units, respectively, until a minimum F value was obtained. The factors θ_{CH}, τ_0/τ_1, and τ_1/τ_2 were then kept constant over the whole temperature range while τ_1 was optimized. The half-angle, θ_{CH_2}, of the librational motion of the C–H vector for the CH_2 carbon was calculated from experimental relaxation data at the minimum and τ_1, τ_0/τ_1, and τ_1/τ_2 values from the CH carbon. Calculations of T_1 and NOE values for the CH_2 carbon at both field strengths over the whole temperature range were performed by entering τ_1, τ_0/τ_1, and τ_1/τ_2 parameters obtained for the CH carbon at a given temperature and the angle θ_{CH_2}.

Theoretical Background

Assuming a purely ^{13}C–^1H dipolar relaxation mechanism,[18] the spin–lattice relaxation time, T_1, and the nuclear Overhauser enhancement, NOE, can be expressed in terms of the spectral density function, $J_i(\omega_i)$, as follows (in the SI system)[19,20]

$$\frac{1}{T_1} = \frac{N}{10}\left(\frac{\mu_0\hbar\gamma_H\gamma_C}{4\pi r^3}\right)^2[J_0(\omega_H - \omega_C) + 3J_1(\omega_C) + 6J_2(\omega_H + \omega_C)] \tag{5}$$

$$\mathrm{NOE} = 1 + \frac{\gamma_H}{\gamma_C}\left[\frac{6J_2(\omega_H + \omega_C) - J_0(\omega_H - \omega_C)}{J_0(\omega_H - \omega_C) + 3J_1(\omega_C) + 6J_2(\omega_H + \omega_C)}\right] \tag{6}$$

where γ_C and γ_H are the magnetogyric ratios of ^{13}C and ^1H nuclei, respectively, μ_0 is the vacuum magnetic permeability, $\hbar = h/2\pi$ where h is Planck's constant, N is the number of directly bonded protons, r is the C–H internuclear distance, and ω_C and ω_H are the ^{13}C and ^1H Larmor frequencies, respectively.

The spectral density function, which is a measure of the distribution of motional frequencies and their intensity, is obtained by Fourier transformation of a time correlation function, $G(t)$, that embodies all of the information about mechanisms and rates of motions

$$J(\omega) = \int_{-\infty}^{+\infty} G(t)e^{i\omega t}\,dt \tag{7}$$

Obtaining $G(t)$ is the crucial point for a quantitative interpretation of the relaxation data. For the simple case of isotropic rotational diffusion, the time correlation function is a single exponential function decaying with a time constant, τ_C, the molecular correlation time

$$G(t) \cong e^{-t/\tau_C} \tag{8}$$

Substituting eq 8 into eq 7 and integrating yield the familiar expression for the spectral density

$$J(\omega) \cong \frac{\tau_C}{1 + \omega^2\tau_C^2} \tag{9}$$

A polymer chain can experience a variety of motions, such as local conformational changes, rotation of the whole chain or tumbling of large segments of the chain at much lower frequencies than the backbone local rearrangements, and motions of pendent groups, e.g., methyl or phenyl. In view of the wide variety of motions with different rates and mechanisms, it is not surprising that eq 9 is an unrealistic model for describing the actual spectral density function for a flexible polymer chain, as is well documented in the literature.[1-3,5,21]

Since the models describing segmental dynamics in flexible polymer chains have been reviewed very comprehensively by Heatley,[1-3] only a short description of the models and the associated spectral densities is given below.

Log χ^2 Distribution Model. This is one of the earliest models interpreting polymeric relaxation data in terms of a distribution of correlation times associated with correlated interactions between repeat units, as well as correlation times in the extreme narrowing region. The spectral

density function for this model is given by[6]

$$J_i(\omega_i) = \int_0^{+\infty} \frac{F(s)\bar{\tau}(b^s - 1)}{(b-1)\left(1 + \omega_i^2\bar{\tau}^2\left[\frac{b^s-1}{b-1}\right]^2\right)} ds \quad (10)$$

where

$$F(s) = \frac{p}{\Gamma(p)}(ps)^{p-1}e^{-ps} \quad (11)$$

is a normalized distribution function. The parameter p is related to the width of the distribution, $\bar{\tau}$ is the average correlation time that defines the center of the distribution, and $\Gamma(p)$ is the gamma function of p and represents a normalization factor. Owing to the use of a logarithmic scale, the variable s is defined by

$$s = \log_b(1 + (b-1)\tau/\bar{\tau}) \quad (12)$$

The logarithmic base is described by the parameter b (usually set to 1000). For $p \geq 100$ this model reduces to the single correlation time model. Note that the distribution function is asymmetric, having a greater density for long correlation times.

Jones–Stockmayer (JS) Model. The JS model originates from the general "tetrahedral or diamond lattice" model first proposed by Valeur and collaborators (VGJM model).[22] The VGJM model is based on three- and four-bond motions, i.e., "crankshaft" motions which are allowed to occur in a polymer chain embedded in a tetrahedral lattice. In solving the lattice equation, which describes the three-bond motion, Valeur et al.[22] used a continuous limit approximation that led to an expression with an unrealistic infinite slope of the resulting time correlation function at $t = 0$. Jones and Stockmayer removed this shortcoming by introducing an arbitrary truncation of the coupling of the motion along the chain. In the absence of overall tumbling and internal rotations of pendent groups the spectral density function of the JS model is given by[7]

$$J_i(\omega_i) = 2\sum_{k=1}^{s} G_k \frac{\tau_k}{1 + \omega_i^2\tau_k^2} \quad (13)$$

$$(\tau_k)^{-1} = w_3\lambda_k \qquad s = (m+1)/2$$

where λ_k and G_k are found from the sharp cutoff solution of the three-bond jump equation as

$$\lambda_k = 4\sin^2\left(\frac{(2k-1)\pi}{2(m+1)}\right) \quad (14)$$

$$G_k = \frac{1}{s} + \frac{2}{s}\sum_{q=1}^{s-1} e^{-\gamma q}\cos\left(\frac{(2k-1)\pi q}{2s}\right) \quad (15)$$

where $\gamma = \ln 9$. The two adjustable parameters in this model are w_3, the characteristic frequency or rate of occurrence for a three-bond jump, that is usually expressed as the harmonic mean correlation time, $\tau_h = (2w_3)^{-1}$, and m, the number of bonds involved in the cooperative motion, or the quantity, $2m-1$, which stands for the chain segment expressed in bonds that are coupled to the central bonds. No correlated motions are assumed outside that segment. The parameter $2m - 1$ represents the breadth of the distribution of correlation times and ensures the aforementioned truncation.

Hall–Weber–Helfand (HWH) Model. This model takes into account correlated pair transitions and isolated transitions occurring with correlation times τ_1 and τ_0, respectively. The pair transitions ensure the propagation along the chain, while isolated, i.e., single-bond transitions, are responsible for damping. The HWH spectral density is given by[8,9]

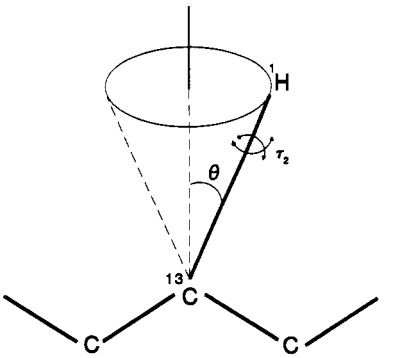

Figure 1. Depiction of the librational motion as described in terms of a random anisotropic fast reorientation of the C–H vector, with a characteristic correlation time τ_2, inside a cone of half-angle, θ, the axis of which is the rest position of the ^{13}C–^{1}H bond.

$$J_i(\omega_i) = 2(\alpha^2 + (-\beta)^2)^{-1/4} + \cos\left(\frac{1}{2}\arctan\left(-\frac{\beta}{\alpha}\right)\right) \quad (16)$$

$$\alpha = \frac{1}{\tau_0^2} + \frac{2}{\tau_0\tau_1} - \omega_i^2 \qquad \beta = -2\omega_i\left(\frac{1}{\tau_0} + \frac{1}{\tau_1}\right)$$

Dejean–Lauprêtre–Monnerie (DLM) Model. While the HWH model represented a significant advance in describing polymer chain local motions, in many cases it was found to underestimate the value of T_1 at the minimum. Furthermore, it could not account for the different local dynamics observed at different carbon sites of a polymer chain.[10,16] The DLM model, which is a clever modification of the HWH model, corrects for these deficiencies by introducing an additional independent motion. This motion is superimposed on the backbone rearrangement, as described by the HWH model, and has been attributed to molecular librations of limited extent of the C–H vector inside a cone of half-angle, θ, the axis of which is the rest position of the C–H bond (Figure 1). This type of librational motion, which must be faster and more local than the orientational diffusion along the chain has been described independently by Howarth.[23] Combining these two models, the composite DLM spectral density is[10]

$$J_i(\omega_i) = \frac{1-A}{(\alpha + i\beta)^{1/2}} + \frac{A\tau_2}{1 + \omega_i^2\tau_2^2} \quad (17)$$

with

$$1 - A = \left[\frac{\cos\theta - \cos^3\theta}{2(1-\cos\theta)}\right]^2 \quad (18)$$

where τ_2 is the correlation time for the librational motion and parameters α and β have been defined in the HWH model.

Results

Figure 2 shows a series of proton-decoupled ^{13}C NMR spectra of PVC in TCE-d_2 recorded at a field strength of 75.4 MHz in the temperature range −19 to +114 °C. As reported earlier by others,[24] both the methine and methylene regions exhibit tacticity effects. Expanded portions of the spectra reveal that at the highest temperature the methine carbon resonance is split so that all ten possible pentads are discernible, with some heptad fine structure, as observed by Elgert.[25] All six possible tetrads are visible in the methylene region, with some hexad fine structure. Since no dependence of T_1 values on stereosequences for

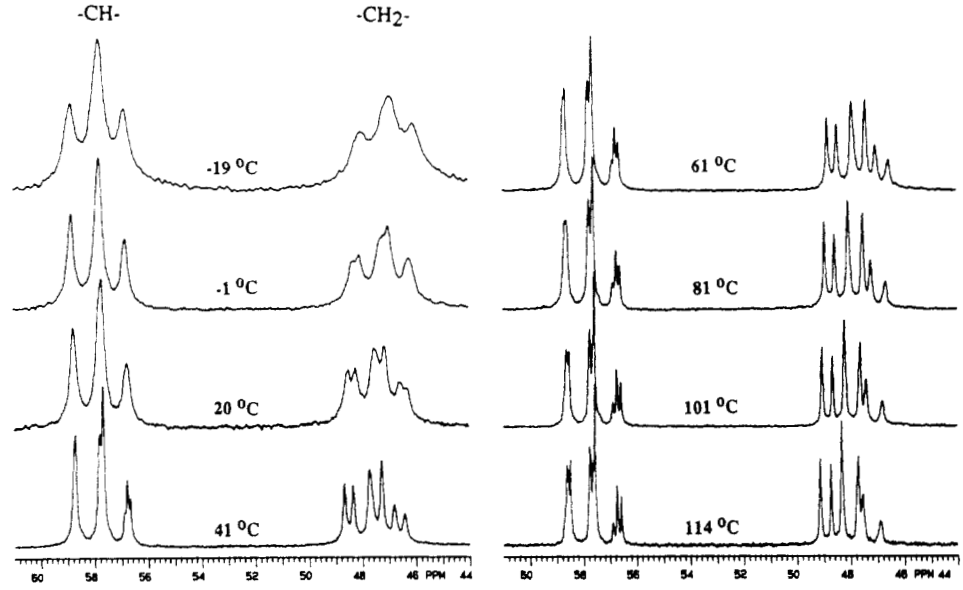

Figure 2. Series of ^{13}C NMR spectra of 5% (w/v) PVC in TCE-d_2 in the temperature range −19 to +114 °C recorded at a magnetic field of 75.4 MHz.

Table I
Experimental Carbon-13 Spin-Lattice Relaxation Times (T_1, ms) and NOE Values[a] of Methine and Methylene Carbons of PVC in DBP and TCE-d_2 as a Function of Temperature at Two Magnetic Fields

	50.3 MHz		75.4 MHz	
temp, °C	CH	CH_2	CH	CH_2
		PVC in DBP		
20	160 (1.43)	83 (1.38)	307 (1.31)	167 (1.28)
41	132 (1.56)	71 (1.50)	226 (1.36)	127 (1.43)
61	136 (1.75)	77 (1.72)	202 (1.54)	114 (1.50)
82	165 (2.06)	92 (2.10)	219 (1.77)	126 (1.79)
91	181 (2.18)	99 (2.16)	241 (1.85)	133 (1.84)
114	264 (2.45)	149 (2.46)	325 (2.16)	183 (2.11)
137	389 (2.54)	222 (2.50)	432 (2.33)	243 (2.23)
		PVC in TCE-d_2		
−19	182 (1.49)	100 (1.55)	290 (1.48)	163 (1.47)
−1	147 (1.55)	81 (1.61)	235 (1.47)	131 (1.49)
20	147 (1.72)	81 (1.71)	214 (1.59)	115 (1.58)
41	172 (1.93)	95 (1.95)	221 (1.66)	124 (1.71)
61	211 (2.18)	115 (2.18)	255 (1.89)	142 (1.96)
81	275 (2.44)	155 (2.51)	315 (1.99)	179 (2.12)
101	374 (2.61)	215 (2.70)	415 (2.18)	232 (2.33)
114	464 (2.65)	266 (2.65)	498 (2.44)	285 (2.47)

[a] Values in parentheses.

poly(vinyl chloride) was found in either solvent and overlapping peaks were observed at low temperatures, average values of T_1 and NOE of the methine and methylene resonances are reported.

Table I summarizes the T_1 and NOE values for the methine and methylene carbons of PVC in DBP and TCE-d_2 as a function of temperature, as determined in the two magnetic fields. Plots of T_1 and NOE values as a function of $1/T$, shown in Figure 3 for PVC in DBP and in Figure 4 for PVC in TCE-d_2, display five characteristics that are commonly observed in relaxation data for polymeric materials: (1) As the temperature decreases, the T_1 values decrease monotonically, in both fields, reaching a minimum which is followed by an increase in T_1 with further decrease in temperature. (2) At a given temperature, T_1 values with increasing magnetic field. The difference in T_1 values between the two magnetic fields becomes more pronounced as the temperature decreases (slow motion regime). (3) The NOE values decrease with increasing magnetic field at all temperatures. (4) Both NOE and T_1 transitions are much broader than for small molecules. (5) At high

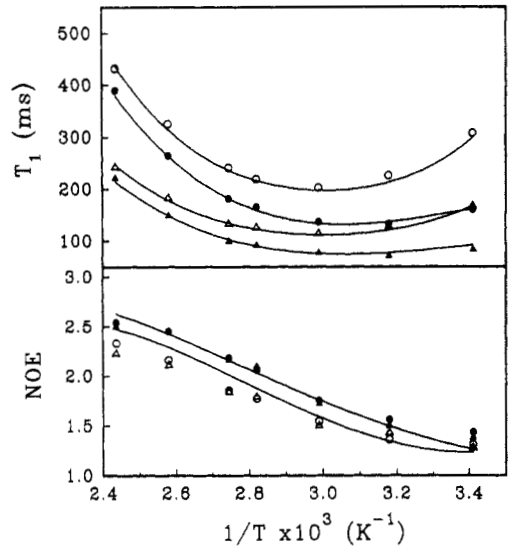

Figure 3. Carbon-13 spin-lattice relaxation times, T_1, and NOE values for methine (circle) and methylene (triangle) carbons of PVC in DBP as a function of reciprocal temperature at field strengths of 50.3 (solid symbols) and 75.4 MHz (open symbols). The solid lines represent the best fit values calculated by the DLM model.

temperatures (fast motion regime), NOE values are substantially less than the theoretical maximum and a residual NOE is observed at low temperatures (slow motion regime).

An interesting feature of the data in Table I is that in both solvents the ratio of T_1 values of the CH and CH_2 groups, $T_1(CH)/T_1(CH_2)$, as determined in both magnetic fields, is fairly constant at 1.80 ± 0.04 throughout the temperature range studied. This value is different from the value 2, which is expected from the number of directly bonded protons and suggests different local motions for the C–H internuclear vectors associated with the CH and CH_2 groups.

Discussion

In modeling the dynamics of PVC two types of motion are considered: (1) the overall tumbling of the entire, or large segments, of the chain and (2) segmental backbone rearrangements. Under the assumption that these motions

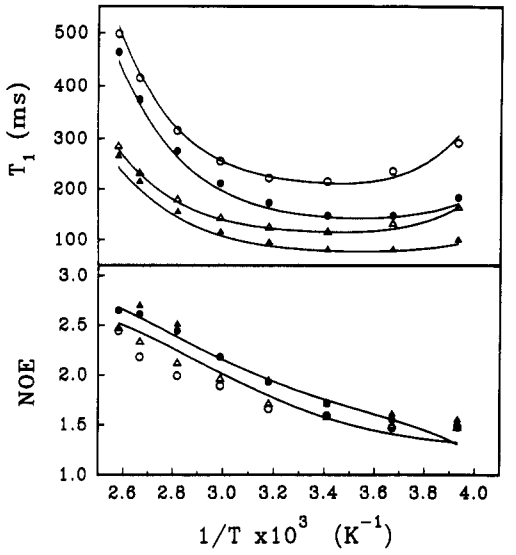

Figure 4. Carbon-13 spin–lattice relaxation times, T_1, and NOE values for methine (circle) and methylene (triangle) carbons of PVC in TCE-d_2 as a function of reciprocal temperature at field strengths of 50.3 (solid symbols) and 75.4 MHz (open symbols). The solid lines represent the best fit values calculated by the DLM model.

act as independent sources of motional modulation of the dipole–dipole interaction, the composite autocorrelation function can be written as a product of the correlation functions associated with each motion. In the event that the overall motion is much slower than the chain local motions, which is usually the case for sufficiently high molecular weight polymers, the overall motion makes a negligible contribution to the relaxation of the backbone carbons.

The correlation time for the overall tumbling of the entire PVC chain, τ_R, at infinite dilution can be estimated from knowledge of the molecular weight, M, and the intrinsic viscosity, $[\eta]$, of the polymer solution in a given solvent with viscosity η_0 through the hydrodynamic equation[26]

$$\tau_R = 2M[\eta]\eta_0/3RT \qquad (19)$$

They were found to be 2.5×10^{-5} s in DBP and 2.4×10^{-6} s in TCE at 30 °C. Such long correlation times guarantee that the local segmental motions are the major source of relaxation for the protonated carbons of PVC in both solvents.

Backbone rearrangement is the second type of motion that modulates dipolar interaction which, as discussed previously, has been modeled by the log χ^2 distribution and HWH, JS, and DLM correlation functions. These four models are evaluated below in their ability to describe the local motions of the PVC chain.

Comparison of Relaxation Data at the T_1 Minimum with Predictions of Motional Models. The first criterion for the validity of any model is the existence of a good fit of relaxation data at the minimum of the curve of T_1 plotted as a function of $1/T$, which corresponds to temperatures of 61 and 20 °C for PVC in DBP and TCE-d_2, respectively. Table II shows the experimentally determined relaxation data for PVC in DBP and TCE-d_2, for the two magnetic fields at a temperature where T_1 exhibits a minimum value, and the calculated relaxation data derived by using the log χ^2, HWH, JS, and DLM correlation functions. The simulation parameters for the four models that best reproduce the relaxation data for both solvents at these temperatures are summarized in Table III.

Table II
Experimental and Calculated[a] (log χ^2, HWH, JS, and DLM Models) Carbon-13 Spin–Lattice Relaxation Times (T_1, ms) and NOE Values[b] of Methine and Methylene Carbons of PVC in DBP and TCE-d_2 for Two Magnetic Fields at a Temperature at Which T_1 Exhibits a Minimum Value

	50.3 MHz		75.4 MHz		
	CH	CH_2	CH	CH_2	σ (%)
			PVC in DBP, 61 °C		
expt	136 (1.75)	77 (1.72)	202 (1.54)	114 (1.50)	
log χ^2	135 (1.68)	68 (1.68)	206 (1.61)	103 (1.61)	2.3
HWH	106 (1.82)	54 (1.82)	154 (1.61)	79 (1.61)	6.8
JS	107 (1.83)	55 (1.83)	154 (1.62)	79 (1.62)	6.7
DLM	136 (1.74)	77 (1.74)	202 (1.55)	114 (1.55)	0.4
			PVC in TCE-d_2, 20 °C		
expt	147 (1.72)	81 (1.71)	214 (1.59)	115 (1.58)	
log χ^2	143 (1.69)	72 (1.69)	218 (1.63)	109 (1.63)	1.7
HWH	109 (1.91)	56 (1.91)	156 (1.71)	80 (1.71)	7.6
JS	107 (1.81)	55 (1.81)	154 (1.60)	79 (1.60)	7.6
DLM	146 (1.75)	80 (1.75)	215 (1.57)	117 (1.57)	0.5

[a] Refer to Table III for simulation parameters. [b] Values in parentheses.

As seen in Table II, for the log χ^2 distribution σ values of 2.3 and 1.7% are obtained for PVC in DBP and in TCE-d_2, respectively. Although these σ values suggest a good fit, a closer examination reveals that this model is unable to account for the relaxation data of both the CH and CH_2 carbons. For example, for PVC in DBP, a distribution width of $p = 11$ yields good agreement between the experimental and calculated data for the CH group whereas the $T_1(CH_2)$ values are underestimated. On the other hand, a distribution width of $p = 10$ results in a better fit for the CH_2 group at the expense of a worse fit for the CH data. This pattern is also followed for the relaxation data of PVC in TCE-d_2. To obtain a good fit for both the CH and CH_2 groups, different p values must be used. This corresponds to a slightly different breadth of correlation times for the CH and CH_2 groups and is the only way that this model can account for the fact that the $T_1(CH)/T_1(CH_2)$ ratio is less than 2. Although this is not a recommended method for fitting the data, it does suggest that these groups may be experiencing different local dynamics. Because this model cannot account for the fact that the $T_1(CH)/T_1(CH_2)$ ratio is less than 2 and models of this type do not provide any precise description of the involved phenomena, it will not be investigated further.

As seen from the high σ values in Table II, it is clear that the HWH and JS models are inadequate in describing the segmental motion of PVC. The high σ values arise from the fact that these models grossly underestimate the value of T_1 at the minimum, and it was mainly for this reason that the DLM model was developed.

The DLM model gives an excellent fit ($\sigma = 0.5\%$) between experimental and calculated T_1 and NOE values for both the CH and CH_2 groups at both fields, making it the best model, by far, in describing the dynamics of PVC in the two solvents. Hence, this model will be used for all further calculations of the relaxation data over the whole temperature range.

PVC Motions According to the DLM Model. The best fit T_1 and NOE data over the whole temperature range for CH and CH_2 carbons of PVC in DBP and in TCE-d_2 are shown graphically in Figures 3 and 4, respectively. It is clear from these plots that very good agreement between experimental and calculated values is obtained from this model throughout the entire temperature range studied. The sole exception is in the values of NOEs at a field strength of 75.4 MHz at the high-temperature

Table III
Simulation Parameters for the log χ^2, HWH, JS, and DLM Models Which Best Reproduce the Relaxation Data of the CH Carbon of PVC in Two Solvents at Temperatures Corresponding to the T_1 Minimum

	log χ^2		HWH		JS		DLM	
solvent	p	$\bar{\tau}$, ns	τ_0, μs	τ_1, ns	$2m-1$	τ_h, ns	τ_0/τ_1	τ_1/τ_2
DBP, 61 °C	11	3.125	10	3.215	7	1.20	7	600
TCE-d_2, 20 °C	9	3.475	10	1.002	7	1.25	7	200

region. For this model the values of the fitting parameter τ_1/τ_2,[27] as shown in Table III, were found to be 600 and 200 for PVC in the DBP and TCE-d_2 solutions, respectively. These ratios indicate that the correlation time for librational motion of the C–H vector of PVC in DBP is 600 times shorter than the correlation time for diffusive chain motions, whereas in TCE-d_2 it is only 200 times shorter.

The best fit half-angles of the librational motion of the C–H vector for the methine carbon, θ_{CH}, and methylene carbon, θ_{CH_2}, were found to be 27 and 32° for PVC in DBP and 30 and 33° for PVC in TCE-d_2. In both solvents θ_{CH} is less than θ_{CH_2} which explains the fact that $T_1(CH)/T_1(CH_2) < 2$ and supports the previous suggestion that the C–H internuclear vectors at the methine and methylene groups experience different local dynamics. The smaller θ value for the CH group indicates a greater steric hindrance to the librational motion of the C–H vector relative to that in the CH_2 group. The methine carbon has a directly attached chlorine atom which, because of its size, physically restricts the amplitude of the local libration. This observation is in agreement with earlier findings for poly(β-hydroxybutyrate)[16,28] and other polymeric systems[10,29,30] that have been summarized by Monnerie.[31]

As seen above, the half-angle of the C–H vector for the methine carbon is smaller for PVC in DBP than in TCE-d_2, i.e., θ_{CH}(in DBP) < θ_{CH}(in TCE-d_2). This result is in agreement with the τ_1/τ_2 ratio in the two solvents; in other words a smaller half-angle should correspond to a shorter correlation time for the librational motion.

It is of interest to note that the values of θ_{CH_2} obtained for PVC in DBP and TCE-d_2 are approximately the same (32 and 33°), whereas those for θ_{CH} (27 and 30°) are quite different. The effects on the quality of the fit for such differences in the librational angle can be seen by comparing the calculated values of T_1 and NOE from the DLM model in Table II, for the two solvents. Examination of these data reveals that the changes in the half-angles do not affect the NOE values; however the T_1 values for the methine carbon change by ~7% whereas the T_1 values for the methylene carbon change by only ~3%. While the percent difference in the T_1 values for the methine carbon are above the usual experimental uncertainty (≤5%), that for the methylene carbon is within this error limit. A smaller half-angle for the methine group in DBP indicates a greater steric hindrance to the librational motion of the C–H vector relative to that of the methine carbon of PVC in TCE-d_2. Such a change in angle could reflect differences in coil dimensions, depending on the solvent quality, or a specific interaction between DBP and the CHCl group of PVC. The latter appears to be more likely since the former should affect the angles of the methine and methylene groups equally. The reduction in θ_{CH} implies that a greater steric hindrance is imposed to the librational motion of the C–H vector, as might be expected from a specific interaction between DBP and the chlorine atom of the PVC chain.

The compatibility of binary mixtures of PVC and plasticizers is generally attributed to the presence of specific interaction(s) between the carbonyl group of the ester and PVC, although the precise nature of these interactions is still a matter of controversy. Infrared spectroscopy studies of blends of ester-containing polymers with PVC as well as solutions of small molecules containing a carbonyl group with PVC or low molecular weight chlorinated molecules have strongly suggested, with general agreement, that the carbonyl group is involved in a specific interaction. However, there has been some debate as to the functional group of PVC with which it is actually interacting. The following specific interactions of the carbonyl group have been suggested: (1) a hydrogen bond with the α-hydrogen,[32-36] i.e., the hydrogen attached to the methine carbon, (2) a hydrogen bond with the β-hydrogens,[37] and/or (3) dipole–dipole interactions with the chlorine atom.[38-40] A hydrogen bond interaction attaches a heavy moiety (DBP) directly to the proton of the ^{13}C–^{1}H vector (Figure 1); such interactions are expected to result in an increase in the half-angle and in a longer correlation time for the librational motion, which is contrary to the observation that a lower value of θ_{CH} and a shorter correlation time (Table III) were obtained for PVC in DBP relative to PVC in TCE-d_2 solution. However, differences in half-angles are in keeping with a complex formation of the type C=O···Cl—C, i.e., between the carbonyl group of DBP and the chlorine atom of PVC.

Table IV
Calculated Correlation Times (τ_1, s) Using the DLM Model To Describe Segmental Motion for the Backbone Carbons of PVC in DBP and in TCE-d_2

PVC in DBP		PVC in TCE-d_2	
temp, °C	$10^9\tau_1$, s	temp, °C	$10^9\tau_1$, s
20	6.241	-19	6.241
41	2.411	-1	2.186
61	1.431	20	1.414
82	0.656	41	0.901
91	0.472	61	0.423
114	0.217	81	0.249
137	0.125	101	0.149
		114	0.109
E_a, kJ/mol	33.4		23.9
$10^{15}\tau_\infty$, s	7.294		72.0
corr coeff (r)	0.998		0.994

[a] Refer to Table III for simulation parameters. [b] Values in parentheses.

The τ_1 values derived from fitting the experimental relaxation data for PVC in both solvents with the DLM model are compiled in Table IV. A plot of the logarithm of these values as a function of $1/T$ shows linear correlations, in the temperature ranges studied, yielding apparent activation energies, E_a, of 33.4 and 23.9 kJ/mol for PVC in DBP and TCE-d_2, respectively. The activation energy, E^*, of the conformational transitions associated with the τ_1 correlation time can be estimated by[41]

$$E^* = E_a - \Delta H_\eta \qquad (20)$$

where ΔH_η is the activation energy for solvent viscosity which was found to be 24.2 and 10.2 kJ/mol for DBP and TCE, respectively. This leads to values of E^* of 9.2 ± 0.9 kJ/mol for PVC in DBP and 13.7 ± 0.9 kJ/mol for PVC in TCE-d_2.

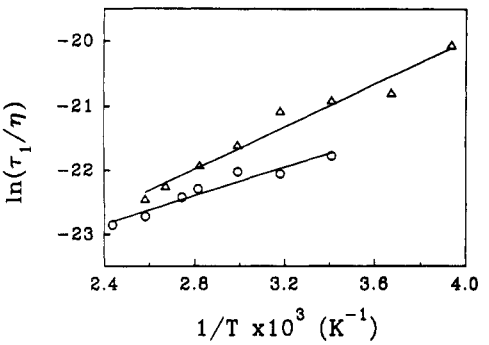

Figure 5. Arrhenius plots of reduced correlation times, τ_1/η, for local segmental motions of PVC in DBP (circle) and in TCE-d_2 (triangle). τ_1 is expressed in nanoseconds and η in centipoise.

The difference in E^* of PVC in the two solvents is in agreement with earlier findings reported by Ediger and co-workers.[42,43] For polyisoprene and polystyrene they found the activation energies were higher for Θ solvents than for good solvents and that local segmental dynamics are slower in Θ solvents. In a Θ solvent the polymer exists in its unperturbed dimensions, i.e., long-range forces between polymer segments which cause the chain to contract are balanced by an expansion caused by polymer–solvent interactions. They suggested that the activation energy obtained for a polymer in a good solvent represents the "true" activation energy associated with rotational barriers traversed in a local conformational change. The local density of segments is higher for a polymer in a Θ solvent which leads to slower local dynamics because the rigid environment inhibits local conformational transitions. It also was pointed out that near the Θ temperature the local segment concentration changes significantly with temperature which adds to the barrier for local chain motions obtained for a good solvent. This is reflected by an increase in the apparent activation energy.

The lower E^* value of PVC in DBP than in TCE suggests that DBP is a better solvent. In addition, the correlation times, τ_1, of the DLM model describing segmental motion (Table IV), scaled by the viscosities of the solvent are longer in TCE than in DBP (Figure 5). This is in agreement with increasing local segment concentration in the poorer TCE solvent. This relative quality of the solvents is also consistent with the Huggins constant, k_H, obtained in this study. These values are 0.36 and 0.74 for PVC in DBP and TCE, respectively. Polymers in Θ solutions exhibit values of k_H close to 0.7, whereas in good solvents the values are much lower, i.e., k_H = 0.2–0.4.[44] Additional evidence for the solvent quality is offered by apparent melting point depression measurements[45] which yielded Flory–Huggins interaction parameters, χ, of –0.22 and +0.34 for PVC with DBP and TCE, respectively.

While the differences in E^* can be accounted for satisfactorily by consideration of solvent quality, the possibility remains that the nature of the local chain motions is different in the two solvents. On the basis of Kramers' equation, Helfand[46] has classified polymer motions into two general types. Type 1 motion is a crankshaft conformational motion about two collinear bonds in which the positions of the chain ends remain unchanged during the transition, while a type 2 motion results in a translational motion of the chain ends, the angular orientation of the two being unaffected. Although the displacement of the chain ends involved in a type 2 motion makes it less favorable than a type 1 motion, a smaller activation energy is associated with the former. In fact the activation energy for a type 2 motion is only slightly greater than the barrier (8–10 kJ/mol) separating the trans and gauche states. Since a type 1 motion involves simultaneous rotations about two coaxial backbone bonds, it involves on the average two barrier crossings (ca. 20 kJ/mol), i.e., twice the energy barrier for the trans–gauche transition. The present experiments indicate an activation energy of 9.2 kJ/mol for the segmental motion of PVC in DBP and, therefore, only a single barrier is crossed, indicating that in this solvent type 2 motions predominate. The higher activation energy (13.7 kJ/mol) for PVC in TCE opens up the possibility that for this solvent type 1 motion may also occur to some degree. Since type 2 motions involve translation of segment ends, they are expected to be more difficult for a contracted coil due to congestion of chain segments than under conditions where the chain dimensions increase, e.g., PVC in DBP. The observed differences in activation energy would then reflect differences in the nature of the chain motions that result from changes in coil dimensions rather than added hindrance to barrier crossing due to local chain interactions. In both cases solvent quality is directly involved. Unfortunately, there is insufficient evidence to choose between these alternative explanations.

Conclusions

Carbon-13 relaxation data of the methine and methylene carbons of PVC in DBP and TCE-d_2 have been modeled by using four different correlation functions describing segmental motion in polymer chains. Among these the log χ^2 failed to account for both the methine and methylene relaxation data and the JS and HWH models failed to account for the T_1 minimum in the curve of T_1 as a function of $1/T$. The DLM model proved to be the superior model and was able to account for the relaxation data of both the methine and methylene carbons of PVC at both field strengths throughout the temperature range studied.

The simulation parameters from this model were found to differ in the two solvents. Firstly, the activation energies for cooperative segmental motion, E^*, in the PVC chain were found to be 9.2 and 13.7 kJ/mol in DBP and TCE-d_2, respectively. The difference in E^* of PVC in the two solvents indicates that DBP is a better solvent for PVC than TCE. Secondly, the half-angle of the C—H vector for the methine carbon is smaller in DBP than in TCE-d_2, reflecting a greater steric hindrance to the librational motion of this vector in DBP. This is rationalized by assuming a specific type of interaction between the carbonyl of the plasticizer and the chlorine atom of PVC, i.e., C=O···Cl—C.

Acknowledgment. Financial assistance in the form of operating grants from the Natural Science and Engineering Research Council (NSERC) and the Government of Québec (Fonds FCAR) is gratefully acknowledged. T.R. would like to thank NSERC, FCAR, and Pall Corp. for postgraduate fellowships. P.D. thanks the University of Crete for granting a leave of absence and Prof. M. D. Ediger for helpful discussions. We are grateful to Ms. Rose Yen for making the viscosity measurements.

References and Notes

(1) Heatley, F. In *Dynamics of Chains in Solution by NMR Spectroscopy*; Booth, C., Price, C., Eds.; Comprehensive Polymer Science; Pergamon Press; New York; 1990; Vol. 1, Chapter 18, p 377.
(2) Heatley, F. *Annu. Rep. NMR Spectrosc.* **1986**, *17*, 179.
(3) Heatley, F. *Prog. Nucl. Magn. Reson. Spectrosc.* **1979**, *13*, 47.
(4) McBrierty, V. J.; Douglass, D. C. *Phys. Rep.* **1980**, *63*, 61.
(5) Schaefer, J. *Top. Carbon-13 Spectrosc.* **1974**, *1*, 150.
(6) Schaefer, J. *Macromolecules* **1973**, *6*, 882.
(7) Jones, A. A.; Stockmayer, W. H. *J. Polym. Sci., Polym. Phys. Ed.* **1977**, *15*, 847.

(8) Hall, C. K.; Helfand, E. *J. Chem. Phys.* **1982**, *77*, 3275.
(9) Weber, T. A.; Helfand, E. *J. Phys. Chem.* **1983**, *87*, 2881.
(10) Dejean de la Batie, R.; Lauprêtre, F.; Monnerie, L. *Macromolecules* **1988**, *21*, 2045.
(11) Sears, J. K.; Darby, J. R. *The Technology of Plasticizers*, Wiley & Sons: New York, 1982.
(12) Titow, W. V. *PVC Technology*, 4th ed.; Applied Science: New York, 1982.
(13) Huggins, M. L. *J. Am. Chem. Soc.* **1942**, *64*, 2716.
(14) Kraemer, E. O. *Ind. Eng. Chem.* **1938**, *30*, 1200.
(15) Dais, P.; Nedea, M. E.; Morin, F. G.; Marchessault, R. H. *Macromolecules* **1989**, *22*, 4208.
(16) Dais, P.; Nedea, M. E.; Morin, F. G.; Marchessault, R. H. *Macromolecules* **1990**, *23*, 3387.
(17) Craik, D. J.; Kumar, A.; Levy, G. C. *J. Chem. Inf. Comput. Sci.* **1983**, *1*, 30.
(18) The preponderence of dipole–dipole relaxation relative to other mechanisms has been examined previously by: Cutnell, J. D.; Glasel, J. A. *J. Am. Chem. Soc.* **1977**, *99*, 42.
(19) Schaefer, J.; Natusch, D. F. S. *Macromolecules* **1972**, *5*, 416.
(20) Doddrell, D.; Glushko, V.; Allerhand, A. *J. Chem. Phys.* **1972**, *56*, 3683.
(21) Heatley, F.; Begum, A. *Polymer* **1976**, *17*, 399.
(22) Valeur, G.; Jarry, J. P.; Gény, F.; Monnerie, L. *J. Polym. Sci., Polym. Phys. Ed.* **1975**, *13*, 667, 675, 2251.
(23) Howarth, O. W. *J. Chem. Soc., Faraday Trans. 2* **1979**, *75*, 853.
(24) Carman, C. J. *Macromolecules* **1973**, *6*, 725. Tonelli, A. E.; Schilling, F. C.; Starnes, W. H.; Shepherd, L.; Plitz, I. M. *Macromolecules* **1979**, *12*, 79.
(25) Elgert, K.-F.; Kosfeld, R.; Hull, W. E. *Polym. Bull.* **1981**, *4*, 281.
(26) Riseman, J.; Kirkwood, J. G. *J. Chem. Phys.* **1949**, *16*, 442. Isihara, A. *Adv. Polym. Sci.* **1968**, *5*, 531.
(27) It is important to note that the ratios τ_1/τ_2 are difficult to determine accurately from the data at the T_1 minimum. In fact good agreement between theory and experiment can be obtained for $50 < \tau_1/\tau_2 < 800$. However, because this ratio influences only the relaxation data in the "long time" or "slow motion" part of the curves, the ratios chosen in this study represent the best fit of relaxation data in this region.
(28) Nedea, M. E.; Marchessault, R. H.; Dais, P. *Polymer* **1992**, *33*, 1831.
(29) Dejean de la Batie, R.; Lauprêtre, F.; Monnerie, L. *Macromolecules* **1988**, *21*, 2045.
(30) Dejean de la Batie, R.; Lauprêtre, F.; Monnerie, L. *Macromolecules* **1988**, *21*, 2052; **1989**, *22*, 122, 2617.
(31) Monnerie, L. *J. Non-Cryst. Solids* **1991**, *131–133*, 755.
(32) Coleman, M. M.; Zarian, J. *J. Polym. Sci., Polym. Phys. Ed.* **1979**, *17*, 837.
(33) Coleman, M. M.; Varnell, D. F. *J. Polym. Sci., Polym. Phys. Ed.* **1980**, *18*, 1403.
(34) Garton, A.; Cousine, P.; Prud'homme, R. E. *J. Polym. Sci., Polym. Phys. Ed.* **1983**, *21*, 2275.
(35) Benedetti, E.; Posar, F.; D'Alessio, A.; Vergamini, P.; Pezzin, G.; Pizzoli, M. *J. Polym. Sci., Polym. Phys. Ed.* **1985**, *23*, 1187.
(36) Varnell, D. F.; Moskala, E. J.; Painter, P. C.; Coleman, M. M. *Polym. Eng. Sci.* **1983**, *23*, 658.
(37) Tremblay, C.; Prud'homme, R. E. *J. Polym. Sci., Polym. Phys. Ed.* **1984**, *22*, 1857.
(38) Heald, C.; Thompson, F. R. S. *Proc. R. Soc London, A* **1962**, *89*, 268.
(39) Tabb, D. L.; Koenig, J. L. *Macromolecules* **1975**, *8*, 929.
(40) Allard, D.; Prud'homme, R. E. *J. Appl. Polym. Sci.* **1982**, *27*, 559.
(41) Kramers, H. A. *Physica* **1940**, *7*, 284.
(42) Waldow, D. A.; Johnson, B. S.; Hyde, P. D.; Ediger, M. D.; Kitano, I.; Ito, K. *Macromolecules* **1989**, *22*, 1345.
(43) Waldow, D. A.; Ediger, M. D.; Yamaguchi, Y.; Matsushita, Y.; Noda, I. *Macromolecules* **1991**, *24*, 3147.
(44) Munk, P. *Introduction to Macromolecular Science*; Wiley & Sons: New York, 1989; p 349.
(45) Anagnostopoulos, C. E.; Coran, A. Y.; Gamrath, H. R. *J. Appl. Polym. Sci.* **1960**, *4*, 181.
(46) Helfand, E. *J. Chem. Phys.* **1971**, *54*, 4651.